J. Fluid Mech. (1977), *vol.* 80, *part* 1, *pp.* 179–202
Printed in Great Britain

Secondary flow due to Alfvén waves

By J. A. SHERCLIFF

Department of Engineering, University
of Warwick, Coventry, England

(Received 2 August 1976)

Large (gigajoule) amounts of energy can in principle be stored as kinetic energy in liquid metal circulating round a torus and can be extracted at the gigawatt level by Alfvén waves propagating along an imposed axial field. A major limitation on the energy that may be so stored is the disruption of these primary Alfvén waves by secondary flows in meridional planes, associated with out-of-balance centrifugal forces ahead of and behind the waves and non-uniform magnetic pressures at the wave fronts. Vorticity, created at the wave, itself propagates in secondary Alfvén waves.

This paper gives a linearized treatment of these secondary motions and the associated perturbations of the imposed axial field and compares the resulting disruption of the primary wave mode with crude estimates made in an earlier paper. The main case treated is the discharge of the stored energy into a matched resistor by an Alfvén step wave but the secondary consequences of standing primary waves are also explored. The nature of the solutions depends on the electromagnetic characteristics of the walls normal to the imposed field. The problem is mathematically interesting because it involves the joint solving of elliptic and hyperbolic equations that are coupled by the boundary conditions at these walls.

1. Introduction

In a recent, speculative proposal (Shercliff 1976) for large (gigajoule) energy-storage devices with liquid-metal rotors, exchanging energy via Alfvén waves, it was recognized that a major limitation on the amount of energy that could be stored was the distortion of the basic wave mode by secondary flow. It is the purpose here to give this problem a fuller treatment that is more accurate and revealing than the crude estimates given in the paper just cited. Being a linearized treatment, however, it applies only to small wave amplitudes whereas any useful energy store would probably involve large amplitudes, for which an analysis of the secondary effects would present a very difficult problem indeed. The secondary effects might themselves be capable of exploitation so as to allow enhanced exchange of kinetic and magnetic energy.

Figure 1 shows the Alfvén energy store at its simplest. The torus formed by rotating the rectangle $WXYZ$ about the z axis is filled with liquid sodium, which is the best liquid conductor. The inner and outer cylinders, of radius r_1 and r_2 respectively, are conducting electrodes and will be taken to be much better conductors than the sodium. The plane top and bottom walls are insulated. A uniform vertical magnetic field B_0 is provided by an external magnet, with flux return through a suitable yoke

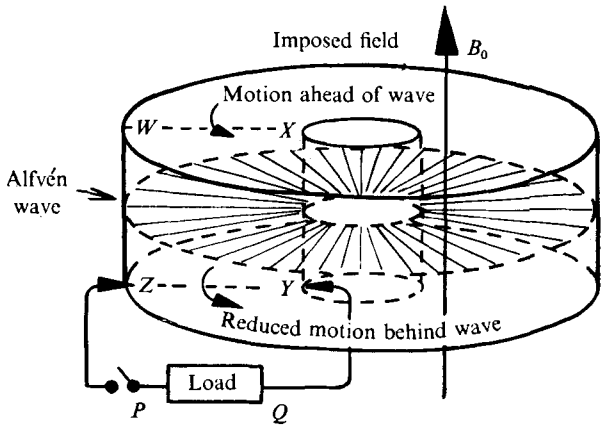

FIGURE 1. Alfvén energy store during discharge.

(not shown). In most of this paper we shall treat the fluid as *virtually* inviscid and perfectly conducting, which is a reasonable first approximation for the very large systems under consideration, as the earlier paper showed. It is moreover still reasonable to treat conducting walls as perfectly conducting in comparison with the sodium provided their resistance is small enough in comparison with that of the relevant skin depths or boundary layers in the sodium.

Energy exchange is achieved via an external circuit connected between the cylindrical electrodes. The figure shows an external circuit PQ schematically. In practice it obviously has to be arranged axisymmetrically, at least in the vicinity of the sodium. One mode of operation is first to apply a slowly rising p.d. across PQ producing radial current flow in the sodium and so causing the liquid rotor to accelerate to a speed that is independent of z but proportional to $1/r$, r being distance from the axis. This occurs because the azimuthal $\mathbf{j} \times \mathbf{B}$ forces are also proportional to $1/r$, as $|\mathbf{j}| \propto 1/r$ in this geometry. 'Slowly rising' here means: rising over a time much longer than the transit time of vertical Alfvén waves in the torus. The current paths are completed by vertical currents in the cylindrical walls.

The stored kinetic energy can then be rapidly extracted at a steady rate by suddenly connecting a resistive load across PQ. The discharge current J initially crosses the liquid as a radial current sheet at the bottom plane $z = 0$, but this sheet promptly propagates upwards as an Alfvén step wave, which reflects at the non-conducting top surface. The wave is a sheet of radial current and vorticity. Since the fluid velocity still varies like $1/r$ at each level, there is no z-wise vorticity. If the load is correctly chosen (i.e. using the matched impedance) each transit of the wave reduces the velocity by one-half of its initial value, leaving behind no kinetic or magnetic energy (other than that of the *vertical* magnetic field) after two transits. After the first transit, one-quarter of the original kinetic energy has been turned into the energy of the azimuthal magnetic field which the initial Alfvén current sheet sets up in its wake. As this is the ideal mode of operation we shall concentrate on this case.

So far we have ignored the fact that the flow is occurring in a curved channel, with vorticity (in the wave sheet) oriented in the direction of curvature, and is therefore prone to secondary flow. Figure 2 records an intuitive appraisal of the situation that occurs when moving fluid containing no azimuthal field is being retarded by the

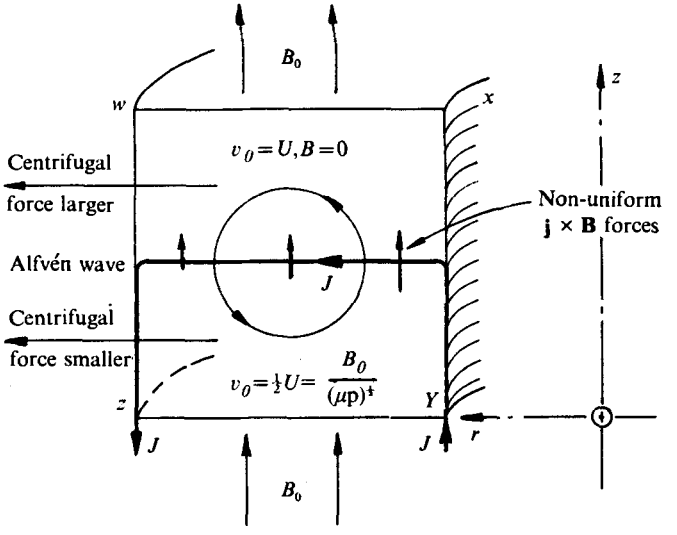

FIGURE 2. Cross-section of left-hand limb of torus.

initial Alfvén step wave. Only the left-hand limb of the torus is shown. The primary velocity v_θ and wave field B_θ are in the $+\theta$ direction, i.e. out of the page, and are proportional to $1/r$. Secondary vorticity would be produced at the wave by the vertical gradient in the radial centrifugal forces and by the radial gradient in the vertical $\mathbf{j} \times \mathbf{B}$ forces in the wave, due to the azimuthal field B_θ created by the wave. The closed loop roughly indicates the resulting secondary motion, which would convect the imposed field B_0 out of shape. The motion and the perturbation of the field would both upset the uniform advance of the primary Alfvén wave. One would expect the azimuthal secondary vorticity produced at the wave itself to propagate vertically in both directions as a secondary system of Alfvén waves, travelling at the same speed as the main wave, and therefore not running ahead of it. Nevertheless, irrotational secondary fluid motion will occur ahead of this wave because that would be caused by *pressure* disturbances which propagate instantaneously, under the usual assumption of incompressibility. This is one of the features that makes this problem particularly interesting; Alfvén wave phenomena are described by mixed elliptic/hyperbolic equations.

One other introductory point is that the secondary flow need not always occur, despite the curvature of the channel. This is because sometimes the magnetic forces or equivalent Maxwell stresses can just balance the centrifugal effects. Consider the advancing wave front referred to axes that are travelling with it z-wards at the Alfvén velocity b ($= B_0/(\mu\rho)^{\frac{1}{2}}$, ρ being the fluid density and μ being $4\pi \times 10^{-7}$ in S.I. units). The motion now obeys the equations of perfect steady MHD:

$$\rho(\mathbf{v}.\mathrm{grad})\,\mathbf{v} + \mathrm{grad}\,p^* = (\mathbf{B}.\mathrm{grad})\,\mathbf{B}/\mu \tag{1}$$

and

$$\mathrm{curl}\,\mathbf{v} \times \mathbf{B} = 0, \tag{2}$$

in which $\mathbf{v}$ and $\mathbf{B}$ are the velocity and magnetic field and p^* is the sum of the pressure p and the magnetic pressure $\mathbf{B}^2/2\mu$. Separating out the term $\mathbf{B}^2/2\mu$ is mathematically convenient but physically very misleading because it makes the magnetic forces

appear to act at the wrong place and in the wrong direction. The right-hand side of (1) can be described as being due to that part of the Maxwell stress which is left after the magnetic pressure has been removed, namely a tension $\mathbf{B}^2/\mu$ along the field lines. The curvature of the azimuthal field lines produces a 'centripetal force' to be set alongside the normal centrifugal effects. As Walén (1944, 1946) pointed out, (1) and (2) can be satisfied exactly by taking one of the cases

$$\mathbf{v} = \pm \mathbf{B}/(\mu\rho)^{\frac{1}{2}} \tag{3}$$

together with $p^* =$ constant, and then the Maxwell tensions can just balance the centrifugal forces and no secondary flow need occur. To get flows relevant to the present discussion we take B_z as B_0 and v_z as $-b$, take v_θ and B_θ to be related by (3), and take v_r and B_r to be zero. If we refer this motion instead to the original axes, relative to which the fluid has no z-wise velocity, so that the wave is advancing at a speed b, then the azimuthal field and velocity must still be proportional, and in particular must vanish together. Such a case occurs if the initial state in figure 2 consists instead of fluid at rest without azimuthal field and an Alfvén wave producing azimuthal flow and field is generated by suddenly applying a voltage and current source across PQ. No secondary flow occurs here during the first transit, even for large amplitude waves.

In general, however, the azimuthal velocity and field are not proportional to each other in accordance with (3), and secondary flow does occur. In particular, secondary flow must occur whenever there are waves travelling in both directions owing to reflexion, etc., for then obviously a Walén flow could not be produced by a change to moving axes.

2. A linearized treatment of the secondary effects

We shall assume that the secondary flows and their associated field perturbations are so weak that (*a*) the primary wave is not significantly affected by them and (*b*) a linearized treatment of the secondary motion is acceptable, i.e. the distance that the secondary motion convects its own vorticity is negligible in the times of interest (typically one or two wave transits). The primary motion is characterized by purely azimuthal velocities v_θ and fields B_θ, each proportional to $1/r$ at each instant and value of z. That $B_\theta \propto 1/r$ is evident from Ampère's law applied to a horizontal circle of radius r centred on the axis, the only vertical currents being in the cylindrical walls.

The secondary phenomenon involves azimuthal vorticity ω_θ associated with velocities v_r and v_z in meridional planes, inducing azimuthal currents j_θ which produce magnetic perturbations B_r and B_z, superposed on the primary field B_0 in the z direction.

The equations of unsteady perfect MHD are

$$\rho\,\partial\mathbf{v}/\partial t + \rho(\mathbf{v}.\operatorname{grad})\,\mathbf{v} + \operatorname{grad} p^* = (\mathbf{B}.\operatorname{grad})\,\mathbf{B}/\mu \tag{4}$$

and

$$\partial\mathbf{B}/\partial t = \operatorname{curl}\mathbf{v}\times\mathbf{B}. \tag{5}$$

Expressed in cylindrical polar co-ordinates with axisymmetry and with quadratic terms in v_r, v_z, B_r and B_z suppressed, these equations have the following components.

(i) *Azimuthal:*

$$\rho\frac{\partial v_\theta}{\partial t} = \frac{B_0}{\mu}\frac{\partial B_\theta}{\partial z}, \quad \frac{\partial B_\theta}{\partial t} = B_0\frac{\partial v_\theta}{\partial z} \tag{6a,b}$$

(i.e. the expected Alfvén wave equations governing the primary flow).

(ii) *Axial:*

$$\rho\frac{\partial v_z}{\partial t}+\frac{\partial p^*}{\partial z}=\frac{B_0}{\mu}\frac{\partial B_z}{\partial z},\quad \frac{\partial B_z}{\partial t}=B_0\frac{\partial v_z}{\partial z}. \tag{7a,b}$$

(iii) *Radial:*

$$\rho\frac{\partial v_r}{\partial t}-\frac{\rho v_\theta^2}{r}+\frac{\partial p^*}{\partial r}=\frac{B_0}{\mu}\frac{\partial B_r}{\partial z}-\frac{B_\theta^2}{\mu r},\quad \frac{\partial B_r}{\partial t}=B_0\frac{\partial v_r}{\partial z}. \tag{8a,b}$$

Equations (7*b*) and (8*b*) express the convection of the field by the secondary motion. As usual, we make progress best in terms of vorticity, having eliminated the unknown pressure. Noting that

$$\omega_\theta=\frac{\partial v_r}{\partial z}-\frac{\partial v_z}{\partial r},\quad \mu j_\theta=\frac{\partial B_r}{\partial z}-\frac{\partial B_z}{\partial r},$$

we deduce wave equations augmented by a source term $\partial P/\partial z$, namely

$$\mu\,\partial j_\theta/\partial t=B_0\,\partial\omega_\theta/\partial z \tag{9}$$

and

$$\frac{\partial\omega_\theta}{\partial t}=\frac{B_0}{\rho}\frac{\partial j_\theta}{\partial z}+\frac{\partial P}{\partial z}, \tag{10}$$

in which $P=(v_\theta^2-B_\theta^2/\mu\rho)/r_m$. For simplicity we shall henceforth assume that the radius ratio r_1/r_2 of the torus is near enough to unity for the variation of r in P to be ignored, the mean value r_m being inserted. One would expect the new vorticity created by the primary waves to split somehow between two trains of secondary waves, travelling in opposite directions. The resulting secondary flow and magnetic field disturbances may be related to ω_θ and j_θ by using stream functions ψ (for flow) and ϕ (for perturbation field) such that, at each instant,

$$\nabla^2\psi=-\omega_\theta,\quad \nabla^2\phi=-\mu j_\theta. \tag{11), (12}$$

Here we take $\nabla^2=\partial^2/\partial r^2+\partial^2/\partial z^2$, the fractional variation of r being assumed small.

The wave equations (9) and (10) and the Poisson equations (11) and (12) have to be solved in parallel, being linked by the boundary conditions on ϕ and ψ at the edge of the cross-section of the torus, which we take to be a square of side $2a$, merely for simplicity.

One condition is that ψ = constant = 0, say, for the edge is a streamline. The other conditions depend on the electromagnetic nature of the environment of the sodium. The cylindrical walls ($r=r_1,r_2$) have already been taken to be perfectly conducting in the z direction and so it is reasonable (though by no means inevitable) to take them as perfectly conducting in the θ direction also. Spontaneous azimuthal currents in them then prevent the z-wise flux linked by either wall from changing and so $\phi=0$ is an appropriate condition for the perturbation field at each wall.

As regards the walls at $z=0$ and $2a$, if they are essentially the faces of a highly permeable magnet yoke, not subject to skin effects and each at constant magnetic potential, the boundary condition is $B_r=0$, i.e. $\partial\phi/\partial z=0$. Then (8) indicates that $\partial v_r/\partial z=0$, i.e. $\partial^2\psi/\partial z^2=0$. Since ψ also vanishes at $z=0$ and $2a$, $\nabla^2\psi$ and ω_θ vanish there too. A consequence is that we may integrate (9) over the cross-section and deduce that

$$\frac{\partial}{\partial t}\iint j_\theta\,dx\,dz$$

vanishes, i.e. the total azimuthal current starts off, and therefore stays, zero.

However, the need for a container to protect the sodium might make the assumption of conducting walls at $z = 0$ and $2a$ a more realistic alternative. Then, to avoid short-circuiting the system, these walls would have to be insulated from the sodium and the cylindrical electrodes. Whatever conductors were being used during discharge to connect the sodium to the external loads (see Shercliff 1976) would also constitute conducting sheets at $z = 0$ and $2a$, although if they had radial slits in them or were a multi-turn 'secondary' winding they would not be capable of carrying azimuthal currents which could control the secondary fields B_r and B_z. The simplest assumption if there are conductors at the top and bottom is to take them as virtually perfect conductors in the azimuthal direction. Then z-wise flux at any radius cannot change and the boundary condition on the magnetic field perturbation becomes $\phi = 0$ on these walls also. The azimuthal electric field then also vanishes, by Faraday s law applied round the torus, and as a consequence v_r must vanish since $\mathbf{E} + \mathbf{v} \times \mathbf{B} = 0$ in the perfectly conducting fluid. The fluid is 'frozen' to the wall. Note that this is an inductive effect and, in this axisymmetric geometry, does not depend on direct electrical contact between the fluid and the wall, which must have an insulated surface, as has already been remarked. The condition $v_r = 0$ implies that $\partial\psi/\partial z = 0$ at $z = 0$ and $2a$.

We shall refer to the cases treated in the previous two paragraphs respectively as '*the magnetic-walls case*' and '*the conducting-walls case*'.

We shall refer our solutions to x, z axes, where $x = r_m - r$. The walls are $x = \pm a$ and $z = 0$, $2a$.

3. Discharge into a matched resistive load

We shall treat in detail this case, in which the liquid, devoid of azimuthal field and initially moving azimuthally at a uniform velocity U (if we ignore variations with radius r), is brought halfway to rest by a plane primary Alfvén step wave that rises from the bottom plane $z = 0$, as indicated in figure 2. Behind this wave there is an azimuthal field $\frac{1}{2}U(\mu\rho)^{\frac{1}{2}}$. In this case, P in (10) is a step wave, travelling with the primary wave, in which P falls from U^2/r_m ahead of the wave to zero behind it. We shall make use of the wave co-ordinates:

$$v = z - bt, \quad w = z + bt - 2a. \tag{13}$$

Whenever the P distribution is any upward-travelling wave, we can put $P = P(v)$ and then (9) and (10) have the general solution

$$-\nabla^2\psi = \omega_\theta = \tfrac{1}{2}t\frac{dP}{dv} - \frac{P}{4b} + g(v,x) + h(w,x) \tag{14}$$

and

$$-\frac{\nabla^2\phi}{(\mu\rho)^{\frac{1}{2}}} = \left(\frac{\mu}{\rho}\right)^{\frac{1}{2}} j_\theta = -\tfrac{1}{2}t\frac{dP}{dv} - \frac{P}{4b} - g(v,x) + h(w,x), \tag{15}$$

in which g and h are as yet unknown complementary functions. dP/dv is the rate of creation of vorticity and (14) shows that just *half* of the vorticity created propagates forwards with the point of its origin, accumulating there in time t to a level $\frac{1}{2}t\,dP/dv$, while the rest propagates backwards, hitting the lower wall. When P is a step wave, dP/dv is a delta function, i.e. the sheet of radial current and vorticity corresponding

to the primary Alfvén wave is also a sheet of azimuthal current and vorticity, whose strength grows linearly in time.

It is convenient at this point to non-dimensionalize the equations by setting

$$\left.\begin{aligned} X = x/a, \quad Z = z/a, \quad T = bt/a, \quad V = v/a, \quad W = w/a, \\ \Psi = r_m b\psi/a^2U^2, \quad \Phi = r_m b\phi/a^2U^2(\mu\rho)^{\frac{1}{2}}. \end{aligned}\right\} \tag{16}$$

We also introduce for convenience a dimensionless function G, which includes the P and g terms in (14) (both functions of v), namely

$$G(V, X) = (bg - \tfrac{1}{4}P)\, r_m/U^2 + \tfrac{1}{4}, \tag{17}$$

and replace h by H, where

$$H(W, X) = bhr_m/U^2 - \tfrac{1}{4}. \tag{18}$$

Then
$$-\nabla^2\Psi = \tfrac{1}{2}T\delta(V) + G + H \tag{19}$$

and
$$-\nabla^2\Phi = -\tfrac{1}{2}T\delta(V) + \tfrac{1}{2}S(V) - G + H, \tag{20}$$

in which ∇^2 is now dimensionless, $\delta(V)$ is a unit delta function at $V = 0$ and $S(V)$ is a unit step function such that $S = 0$ for $V > 0$ but $S = 1$ for $V < 0$. The Poisson equations (19) and (20) cannot be solved directly because G and H are unknown. They are determinable, however, because Ψ has to satisfy *two* boundary conditions ($\Psi = 0$ and $\partial\Psi/\partial Z = 0$ or $\partial^2\Psi/\partial Z^2 = 0$) at $Z = 0$ or 2, i.e. more than the norm for a Poisson equation. The extra conditions in effect generate fresh waves by electromagnetic induction and these propagate into the liquid from the top and the bottom, providing the necessary distributions of G and H. These distributions are a function of the previous history, because of the delays associated with the wave motion. The problem is seen to be a particularly interesting mixed elliptic/hyperbolic one. Ψ has to be found first and subsequently Φ is easily deduced, G and H then being known.

As there is no secondary motion or perturbation field at $T = 0$, $G+H$, $-G+H$ and so also G and H all vanish for the relevant ranges of V and W, namely $0 \leqslant V \leqslant 2$ and $-2 \leqslant W \leqslant 0$, within the fluid.

It turns out that the magnetic-walls case is much the easier to solve and we shall therefore take it first. We shall initially consider only the first transit of the waves, i.e. $0 \leqslant T \leqslant 2$.

4. The magnetic-walls case

The controlling boundary conditions are $\Psi = 0$ at $Z = 0$, 2 or at $X = \pm 1$, and also $\nabla^2\Psi = 0$ at $Z = 0$, 2. The latter condition, together with (19), implies for $0 < T \leqslant 2$ that (*a*) at $Z = 0$, where $-2 \leqslant W \leqslant 0$ (and so $H = 0$) and $-2 \leqslant V \leqslant 0$, $G = 0$ for $-2 \leqslant V \leqslant 0$ also, while (*b*) at $Z = 2$, where $0 \leqslant V \leqslant 2$ (and so $G = 0$) and $0 \leqslant W \leqslant 2$, $H = 0$ for $0 \leqslant W \leqslant 2$ also. Physically, (*a*) implies that the requirement that the magnetic field should stay normal to the poleface has the effect that reflected waves are continually generated which, in this case, result in the suppression of all the vorticity shed behind the primary wave, while (*b*) implies not only that there is no vorticity ahead of the primary wave but also that the top boundary does not emit waves of vorticity either, a result which seems totally unsurprising until one has met the conducting-walls case, which follows later.

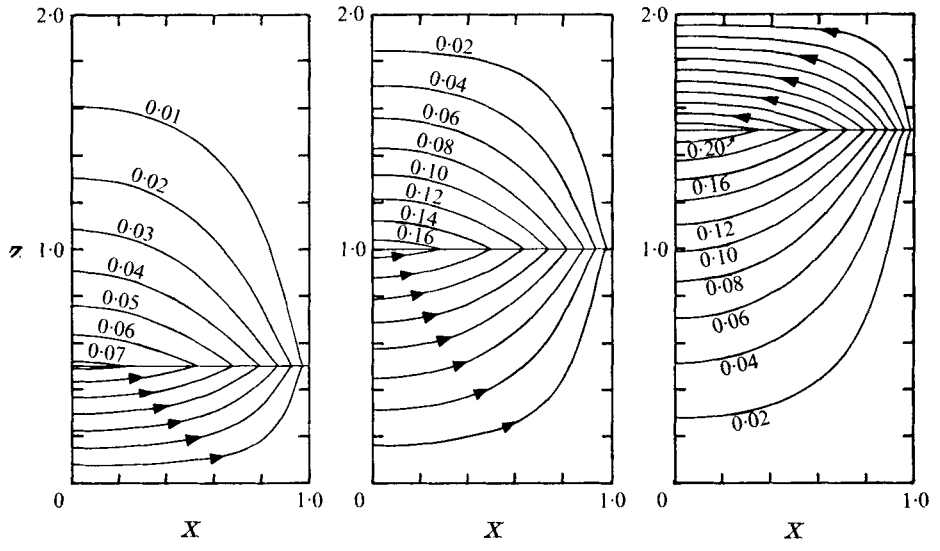

FIGURES 3 (*a–c*). For legend see facing page.

As a result (19) becomes merely

$$-\nabla^2\Psi = \tfrac{1}{2}T\delta(V) \tag{21}$$

while (20) becomes

$$-\nabla^2\Phi = -\tfrac{1}{2}T\delta(V) + \tfrac{1}{2}S(V). \tag{22}$$

Solutions may be found as Fourier series with respect to either X or Z. The choice of X is more convenient for computing purposes and will be preferred. (This choice is essential in the conducting-walls case.) Subject to the conditions $\Psi = \Phi = 0$ at $X = \pm 1$ and $\Psi = \partial\Phi/\partial Z = 0$ at $Z = 0, 2$, the solutions are

$$\Psi = \begin{cases} T\Sigma \dfrac{(-1)^{n-1}}{N^2} \dfrac{\cos NX \sinh N(2-Z) \sinh NT}{\sinh 2N} & \text{if} \quad V \geqslant 0, \quad Z \geqslant T, \\ T\Sigma \dfrac{(-1)^{n-1}}{N^2} \dfrac{\cos NX \sinh N(2-T) \sinh NZ}{\sinh 2N} & \text{if} \quad V < 0, \quad Z < T, \end{cases} \tag{23}$$

in which $N = \frac{1}{2}(2n-1)\pi$ and n takes all positive integral values, and

$$\Phi = \begin{cases} \left.\begin{aligned} &-T\Sigma \frac{(-1)^{n-1}}{N^2} \frac{\cos NX \cosh N(2-Z) \cosh NT}{\sinh 2N} \\ &+\Sigma \frac{(-1)^{n-1}}{N^3} \frac{\cos NX \cosh N(2-Z) \sinh NT}{\sinh 2N} \end{aligned}\right\} \text{if} \quad V \geqslant 0, \quad Z \geqslant T, \\ \left.\begin{aligned} &-T\Sigma \frac{(-1)^{n-1}}{N^2} \frac{\cos NX \cosh N(2-T) \cosh NZ}{\sinh 2N} \\ &+\Sigma \frac{(-1)^{n-1}}{N^3} \cos NX \left(1 - \frac{\sinh N(2-T) \cosh NZ}{\sinh 2N}\right) \end{aligned}\right\} \text{if} \quad V < 0, \quad Z < T. \end{cases} \tag{24}$$

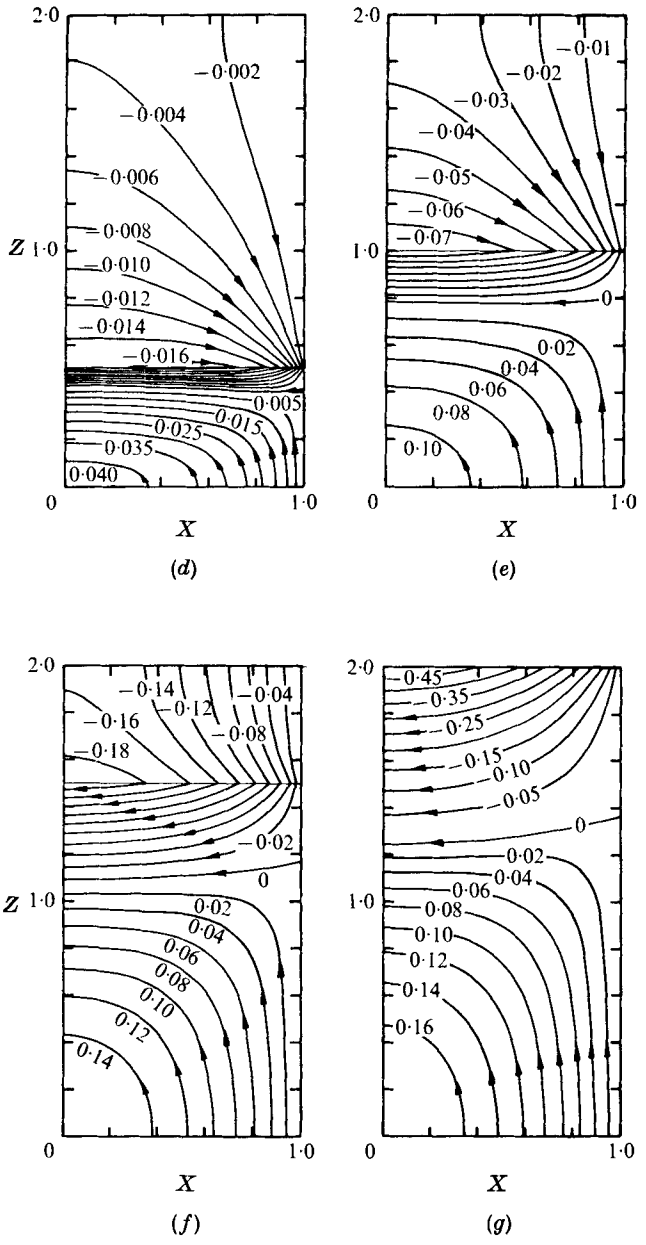

FIGURE 3. Magnetic-walls case. (*a*)–(*c*) Streamlines and (*d*)–(*g*) perturbation field lines in right-hand half of left-hand limb of torus. The numerical values refer to Ψ and Φ. (*a*), (*d*) $T = 0{\cdot}5$. (*b*), (*e*) $T = 1{\cdot}0$. (*c*), (*f*) $T = 1{\cdot}5$. (*g*) $T = 2{\cdot}0$.

In this case the motion consists of two irrotational regions separated by a vortex sheet. By Stokes' theorem the closed-loop streamlines must all intersect the sheet. The ends of the vortex sheet at $X = \pm 1$ are singular because the necessary jump in horizontal velocity v_r across the sheet is inconsistent with the boundary condition $v_r = 0$ and consequently $v_z \to \infty$ there. This singularity is an artificial consequence of

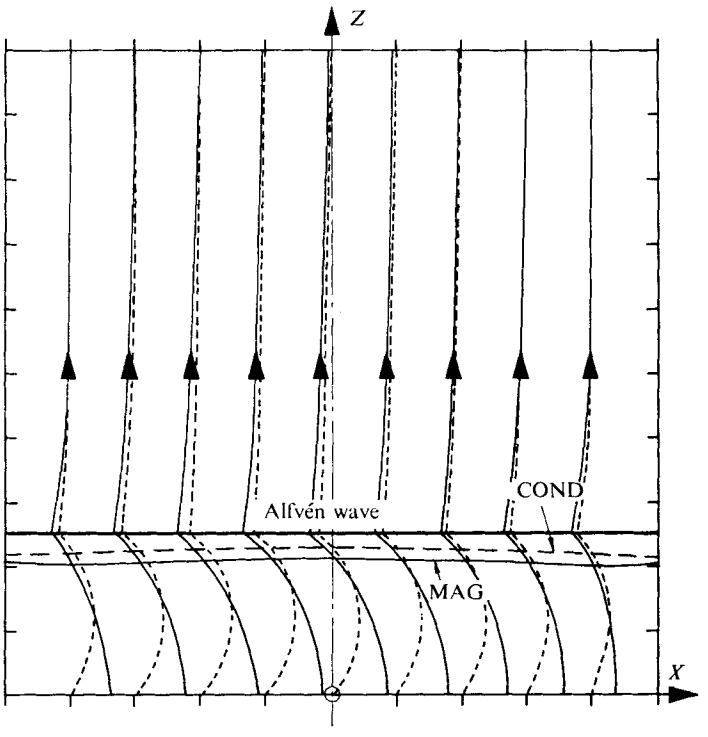

FIGURE 4. Perturbation of imposed field B_0 by secondary field when $T = 0{\cdot}5$ and $B_0 = aU^2(\mu\rho)^{\frac{1}{2}}/4br_m$. ——, magnetic-walls case; – – –, conducting-walls case.

assuming zero dissipation, and would be eliminated if one allowed for small but finite resistivity. This would lead to a wave layer of finite thickness and also finite boundary layers on the walls at $X = \pm 1$ if the side walls were made finitely conducting. Even then the linearizing assumptions that the secondary flow did not significantly affect the primary wave or convect its own vorticity far would fail first in these vicinities, where the velocities would still reach their greatest values. Exactly parallel considerations apply to the magnetic side of the problem. In this approximation the total vertical field falls past zero and reverses at one end of the wave.

Representative streamline and perturbation field line patterns are presented for $T = 0{\cdot}5$, $1{\cdot}0$, $1{\cdot}5$ and $2{\cdot}0$ in figure 3. There is no flow at $T = 2{\cdot}0$ (and hence no streamline picture) but azimuthal currents and perturbations of the field still persist in this case (figure 3*g*). The vortex sheet is growing in strength and so the secondary flow accelerates until the influence of the vortex sheet is inhibited (and finally extinguished at $T = 2$) by the top wall. The maximum value of Ψ is about $0{\cdot}215$, occurring at $X = 0, Z = T$ (i.e. the centre of the wave) when T is approximately $1{\cdot}45$. This indicates that the average secondary vertical velocity reaches a maximum value of about $0{\cdot}215aU^2/br_m$. (This should be compared with the crude estimate of $aU^2/\pi br_m$ given in the earlier paper, Shercliff 1976.) The average horizontal velocity above the wave at $T = 1{\cdot}45$ is about twice as large.

In figure 3(*g*) the fact that the perturbation field is not normal to the wall at $Z = 2$ is attributable to the current sheet which is just reaching this wall.

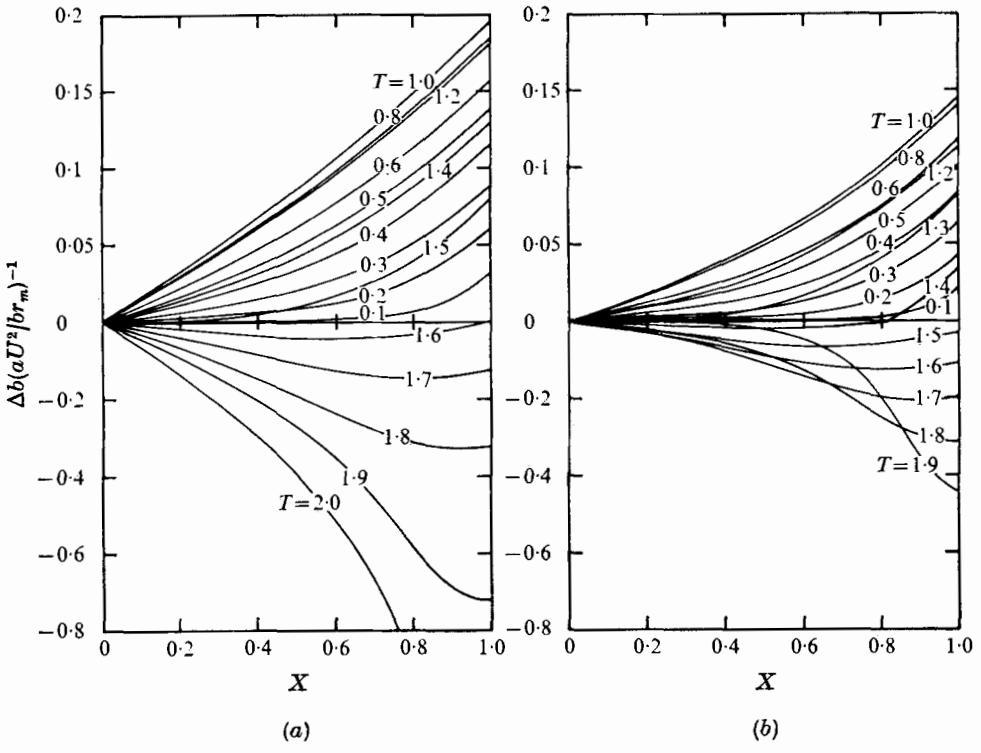

FIGURE 5. Perturbation of primary wave velocity. (*a*) Magnetic-walls case. (*b*) Conducting-walls case. The scale changes for negative values.

It is interesting to compare the convected field shape with expectation. At the risk of overstepping the range where linearization is wholly valid so as to make the effects clearly visible, figure 4 shows typical total field lines that result from combining the perturbation field at $T = 0{\cdot}5$ with an original uniform vertical field chosen to be of strength $\frac{1}{4}aU^2(\mu\rho)^{\frac{1}{2}}/br_m$. The label 'MAG' indicates for the magnetic-walls case the line $\Phi = 0$, on which the original field lines have moved neither left nor right. As expected from a consideration of the flow patterns, the field lines below this line have moved to the right while the weaker flows above the wave have moved the field lines to the left, but to a much smaller extent. There is no contradiction in the region between the wave and the line $\Phi = 0$ because here there is fluid which earlier had spent more time above than below the wave and therefore leftward displacement is possible. The field stays normal to the top and bottom walls.

The convection of the field has the effect of strengthening the vertical field at the wave on the left and weakening it on the right, with corresponding effects on the Alfvén speed. It will be noticed that this effect and the direct convection of the primary Alfvén wave by the vertical velocities are to some extent mutually compensating. For instance, on the right the wave rises more slowly relative to fluid which is itself rising. The resulting increase in the absolute upward vertical velocity of the primary Alfvén wave is

$$\Delta b = -\frac{aU^2}{br_m}\frac{\partial}{\partial X}(\Psi + \Phi) \tag{25}$$

evaluated at $Z = T$, which is given by the equation

$$\left.\begin{aligned} \Delta b &= aU^2/br_m \Sigma(-1)^{n-1} Q \sin NX, \\ \text{in which} \quad Q &= [(\cosh N(2-T)\sinh NT)/N - T\cosh 2N(T-1)]/N\sinh 2N. \end{aligned}\right\} \tag{26}$$

Convergence is much slower at $T = 2$ and Δb then tends to infinity as $X \to 1$. Appendix B gives a convenient approximation for this case. The average ($0 \leqslant X \leqslant 1$) value Δb_m takes the following values:

$T =$	0·2	0·4	0·6	0·8	1·0
$\Delta b_m(aU^2/br_m)^{-1} =$	0·0148	0·0423	0·0671	0·0837	0·0899
$T =$	1·2	1·4	1·6	1·8	2·0
$\Delta b_m(aU^2/br_m)^{-1} =$	0·0818	0·0499	−0·0267	−0·1885	−0·4955

From this we may infer that the perturbation of the primary Alfvén wave is not serious until T approaches 2 if $0{\cdot}09aU^2/br_m \ll b$, i.e. secondary effects are negligible if $ar_m^{-1}(U/b)^2 \ll 11$, say. This should be compared with the criterion $ar_m^{-1}(U/b)^2 \ll \pi$ which was arrived at by crude arguments in the earlier work (Shercliff 1976). This is now seen to be unduly pessimistic, the reason being that the compensatory effect of the field distortion was ignored in that paper. The perturbation gets much worse as $T \to 2$, however, when $\Psi \to 0$ but Φ does not. For this reason the conducting-walls conditions give much better performance.

It is particularly noteworthy that the partial compensation between the terms $\partial\Psi/\partial X$ and $\partial\Phi/\partial X$ includes a cancelling of the terms which increase without limit as $X \to \pm 1$, so that the increase in wave velocity stays finite there. This gives increased confidence in the validity of results given here. Figure 5(*a*) shows how $\Delta b(aU^2/br_m)^{-1}$ varies with T and X, reaching a maximum around $T = 1{\cdot}0$ and later increasing negatively as $T \to 2$. Note the change of scale for negative values.

5. The conducting-walls case

Again we consider the first transit of the wave ($0 \leqslant T \leqslant 2$) at this stage. The controlling boundary conditions are $\Psi = 0$ at $Z = 0$, 2 or at $X = \pm 1$ and also $\partial\Psi/\partial Z = 0$ at $Z = 0, 2$. $\nabla^2\Psi$ consists of three terms:

$$-\nabla^2\Psi = \tfrac{1}{2}T\delta(V) + G(V,X) + H(W,X). \tag{27}$$

We proceed by seeking a solution consisting of four terms, namely

$$\Psi = U'(X,Z,T) + Q'(V,X) + R'(W,X) + A'(X,Z,T), \tag{28}$$

with the following characteristics.

(*a*) U', Q', R' and A' all vanish at $X = \pm 1$ and at $T = 0$ ($0 \leqslant Z \leqslant 2$).

(*b*) U' vanishes also at $Z = 0, 2$ and is determined by the equation $-\nabla^2 U' = \tfrac{1}{2}T\delta(V)$.

(*c*) Q' and R' are zero for $V \geqslant 0$ and $W \leqslant 0$ respectively, to satisfy the requirement that G (which equals $-\nabla^2 Q'$) and H (which equals $-\nabla^2 R'$) vanish ahead of the waves emanating from the bottom and top walls.

(*d*) A' is a harmonic function which does not contribute to $\nabla^2\Psi$ and serves to enable Ψ to vanish at $Z = 0, 2$.

(*e*) The four functions can be expressed as Fourier series in X of the forms

$$\left.\begin{aligned} U' &= \Sigma \frac{(-1)^{n-1}}{4N^3} U(Z,T)\cos NX, \\ Q' &= \Sigma \frac{(-1)^{n-1}}{4N^3} Q(V)\cos NX, \\ R' &= \Sigma \frac{(-1)^{n-1}}{4N^3} R(W)\cos NX, \\ A' &= \Sigma \frac{(-1)^{n-1}}{4N^3} A(Z,T)\cos NX. \end{aligned}\right\} \tag{29}$$

Again $N = \frac{1}{2}(2n-1)\pi$, n takes all positive integral values and the factor $(-1)^{n-1}/4N^3$ is chosen for convenience. Characteristics (*b*) above lead to the results

$$U = \begin{cases} 4NT\dfrac{\sinh N(2-Z)\sinh NT}{\sinh 2N} & \text{if} \quad V \geqslant 0, \\ 4NT\dfrac{\sinh N(2-T)\sinh NZ}{\sinh 2N} & \text{if} \quad V < 0. \end{cases} \tag{30}$$

Characteristics (*d*) determine A in terms of Q and R, as follows:

$$A = -\frac{Q(-T)\sinh N(2-Z) + R(T)\sinh NZ}{\sinh 2N}, \tag{31}$$

for U vanishes at $Z = 0, 2$, R vanishes at $Z = 0$, Q vanishes at $Z = 2$, $V = -T$ at $Z = 0$ and $W = T$ at $Z = 2$.

All conditions have now been satisfied except the crucial, wave-generating conditions on $\partial\Psi/\partial Z$ at $Z = 0, 2$.

If we let $P(T) = Q(-T)$, then at $Z = 0$

$$V = -T, \quad \frac{\partial Q}{\partial Z} = \frac{dQ}{dV} = -\frac{dP}{dT},$$

while at $Z = 2$

$$W = T, \quad \frac{\partial R}{\partial Z} = \frac{dR}{dW} = \frac{dR(T)}{dT}.$$

Hence, for each set of Fourier components, the two $\partial\Psi/\partial Z$ conditions become the coupled, first-order, differential equations

$$\left.\begin{aligned} &4N^2T\frac{\sinh N(2-T)}{\sinh 2N} - \frac{dP}{dT} - \frac{N(-P\cosh 2N + R)}{\sinh 2N} = 0 \quad (\text{at } Z = 0) \\ \text{and} \quad &-4N^2T\frac{\sinh NT}{\sinh 2N} + \frac{dR}{dT} - \frac{N(-P + R\cosh 2N)}{\sinh 2N} = 0 \quad (\text{at } Z = 2). \end{aligned}\right\} \tag{32}$$

Choosing the appropriate constants in the resulting complementary functions to meet the requirement that P (or Q) and R vanish at $T = 0$, we deduce that

$$P(T) = Q(-T) = 4NT\sinh NT - 2\cosh NT - 2(\sinh^2 N)\exp(NT\coth N) + 2(\cosh^2 N)\exp(NT\tanh N)$$

and

$$R(T) = -2\cosh N(T+2) + 2(\sinh^2 N)\exp(NT\coth N) + 2(\cosh^2 N)\exp(NT\tanh N);$$

and A is now determined. Moreover, substituting $-V$ for T in the first equation and W for T in the second yields the desired expressions for $Q(V)$ and $R(W)$, provided $V < 0$ or $W > 0$, respectively. (Q and R vanish for $V \geqslant 0$ or $W \leqslant 0$ respectively, it will be remembered.)

The solution for Ψ for $0 \leqslant T \leqslant 2$ has now been completely found but for brevity we shall not present it complete at this point. At first sight it appears to be an extravagantly divergent series because of terms containing $\sinh NT$ or $\exp(NT\coth N)$, etc. In fact all these quantities, which increase very rapidly without limit as N increases, largely cancel each other, leaving only terms which *diminish* with increasing N. Convergence is actually quite rapid, being slowest in the case $Z = T$ ($V = 0$), where the series goes like $1/N^2$. For computing purposes it is absolutely essential to replace the exact solution by an asymptotic form valid at high N, and this is given in appendix A. In practice the exact form is acceptable only for the *first* terms ($N = \frac{1}{2}\pi$), and even for $N = \frac{3}{2}\pi$ as well as for all higher terms the asymptotic form is much more accurate!

Once Ψ has been found, Φ may be deduced. Inspection of (19) and (20) reveals that Φ may be written down by taking

$$\Phi = -U' - Q' + R' + C' + B', \tag{33}$$

in which the change of sign of U' and Q' as compared with Ψ accommodates the change of sign of the δ and G terms in (20), as compared with (19). Here C' is a solution of the equation $-\nabla^2\Phi = \frac{1}{2}S(V)$, vanishing at $X = \pm 1$ and $Z = 0, 2$, and B' is a new harmonic function enabling Φ to vanish at $Z = 0, 2$ in the face of non-zero values of Q' and R' there.

Now we let

$$C' = \Sigma \frac{(-1)^{n-1}}{4N^3}(\cos NX)\, C(Z, T),$$

and find that

$$C = \begin{cases} \dfrac{4(\cosh NT - 1)\sinh(2-Z)}{\sinh 2N} & \text{if} \quad V \geqslant 0, \\ 4\left(1 - \dfrac{\cosh N(2-T)\sinh NZ + \sinh N(2-Z)}{\sinh 2N}\right) & \text{if} \quad V < 0. \end{cases} \tag{34}$$

Letting

$$B' = \Sigma \frac{(-1)^{n-1}}{4N^3}(\cos NX)\, B(Z, T)$$

leads to

$$B = \frac{Q(-T)\sinh N(2-Z) - R(T)\sinh NZ}{\sinh 2N}. \tag{35}$$

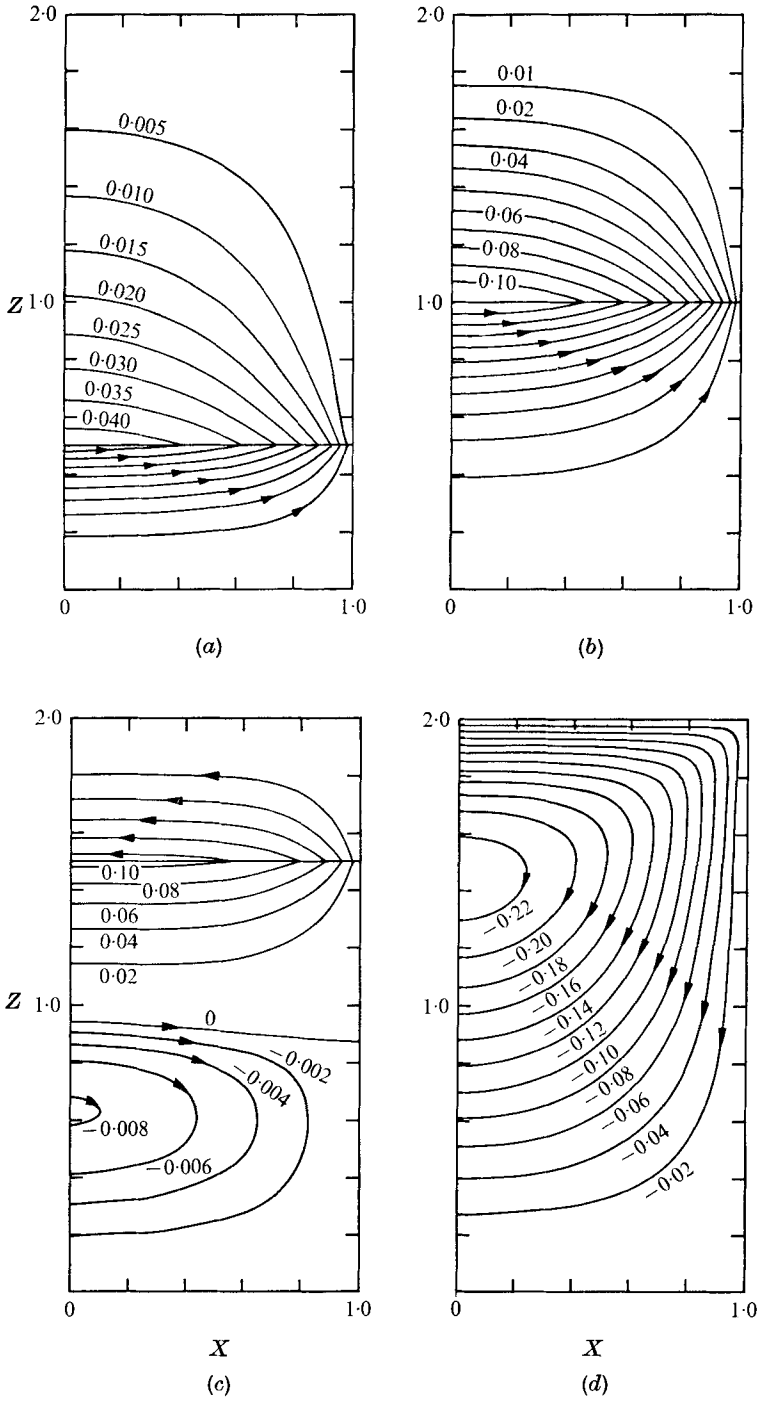

FIGURES 6 (*a–d*). For legend see page 194.

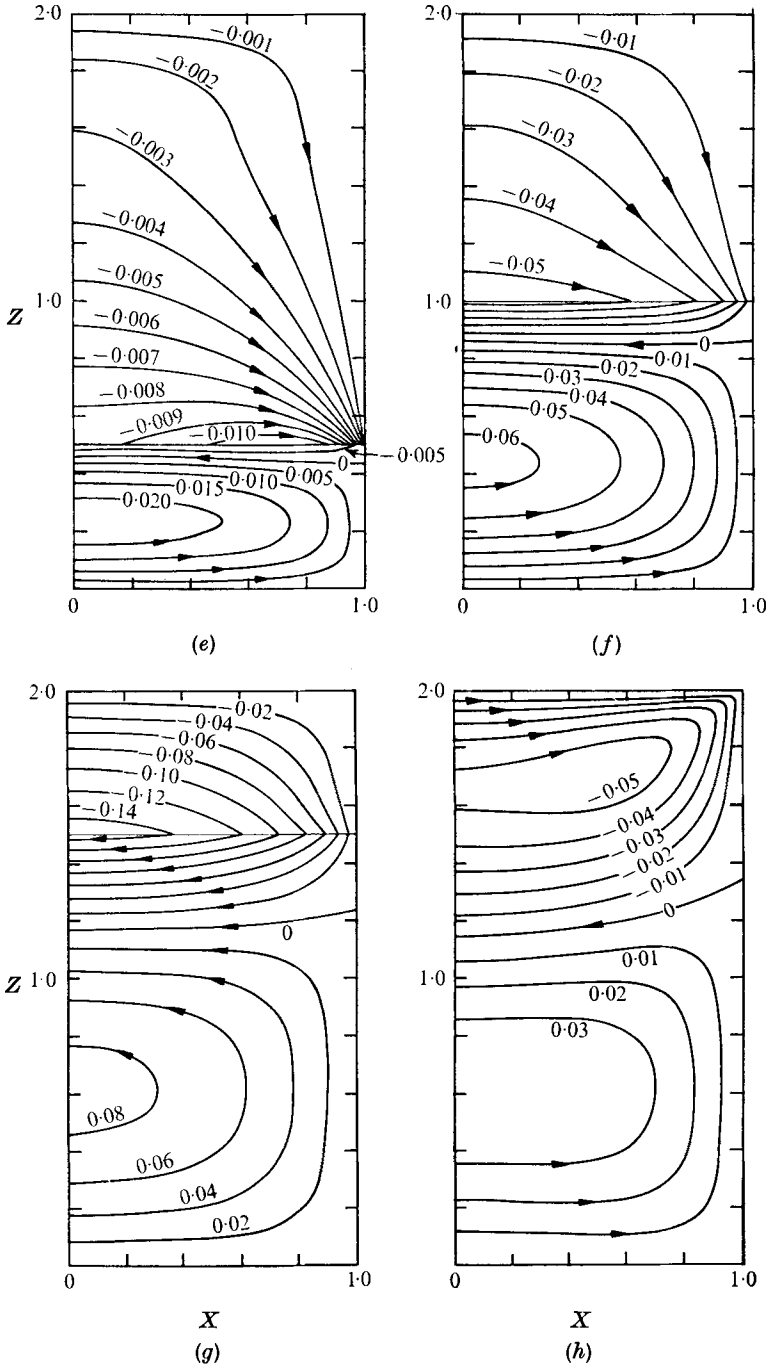

FIGURE 6. Conducting-walls case. (*a*)–(*d*) Streamlines and (*e*)–(*h*) perturbation field lines in right-hand half of left-hand limb of torus. The numerical values refer to Ψ and Φ. (*a*), (*e*) $T = 0{\cdot}5$. (*b*), (*f*) $T = 1{\cdot}0$. (*c*), (*g*) $T = 1{\cdot}5$. (*d*), (*h*) $T = 2{\cdot}0$.

For Φ, as for Ψ, an asymptotic form must be used except when $N = \frac{1}{2}\pi$, and appendix A lists the appropriate formulae for computing.

As with the magnetic-walls case, the solutions in this approximation are singular at the ends ($X = \pm 1$) of the primary wave ($Z = T$), and the secondary velocity and field perturbation increase without limit there.

Representative streamline and perturbation field line patterns are presented for $T = 0{\cdot}5$, $1{\cdot}0$, $1{\cdot}5$ and $2{\cdot}0$ in figure 6. In contrast to the magnetic-walls case, flow persists at $T = 2{\cdot}0$ because of the fresh vorticity propagated into the interior from the top and bottom walls. The maximum *positive* value of Ψ is about $0{\cdot}128$, occurring at the centre of the wave when T is approximately $1{\cdot}25$, but a larger *negative* value ($-0{\cdot}229$) occurs when $T = 2$ at $X = 0$, $Z = 1{\cdot}45$, approximately. Here the braking effect of the top conducting wall is instantaneously suspended as the vortex sheet reaches it. Otherwise the secondary velocities are generally less than in the magnetic-walls case, owing to the braking effect of the conducting walls. The sparsity of the streamlines near $Z = 0, 2$ in figures 6 (*a*)–(*c*) is evidence of this. Figure 6 (*c*), showing the streamlines when $T = 1{\cdot}5$, is considerably more complex than the corresponding magnetic-walls case (figure 3*c*). Sufficient reversed vorticity has been emitted by the lower wall to cause closed eddies of opposite circulation, and only such eddies survive as $T \to 2$. A strong flow results.

It is noteworthy that the onset of the wave of vorticity and current emitted by the top wall is very gentle and is not obviously detectable in the figures, except perhaps in figure 6 (*e*), at the level $Z = 1{\cdot}5$, the head of this wave. In this figure only some of the upper perturbation field lines have been plotted just below the primary wave, for clarity.

The general behaviour of the magnetic field is not greatly different from that in the magnetic-walls case, apart from the absence of perturbations at $Z = 0$ and 2. For comparison with the magnetic-walls case figure 4 shows how the total magnetic field has been convected up to $T = 0{\cdot}5$ in the conducting-walls case, where the original imposed field is again $\frac{1}{4}aU^2(\mu\rho)^{\frac{1}{2}}/br_m$. The label 'COND' indicates the line where $\Phi = 0$ and the original field lines have moved neither right nor left. The 'tethering' of the field lines by the conducting top and bottom walls is now apparent. Once again there is a zone of 'reverse' convection just below the primary wave for the same reasons as in the magnetic-walls case. It turns out that it is somewhat smaller at each instant in the conducting-walls case.

As in the magnetic-walls case, the final effect Δb on the upward velocity of the primary Alfvén wave is the outcome of two competing effects, the vertical velocity of the fluid and the perturbation of the vertical field, and is given again by (23) with appropriate values for Φ and Ψ inserted. (See appendix B.) Now Δb falls to zero as T approaches 2 because any field perturbation there is suppressed by the conducting walls. The average value Δb_m takes the following values:

$T =$	$0{\cdot}2$	$0{\cdot}4$	$0{\cdot}6$	$0{\cdot}8$	$1{\cdot}0$
$\Delta b_m(aU^2/br_m)^{-1} =$	$0{\cdot}0080$	$0{\cdot}0250$	$0{\cdot}0431$	$0{\cdot}0565$	$0{\cdot}0589$
$T =$	$1{\cdot}2$	$1{\cdot}4$	$1{\cdot}6$	$1{\cdot}8$	$2{\cdot}0$
$\Delta b_m(aU^2/br_m)^{-1} =$	$0{\cdot}0398$	$-0{\cdot}0081$	$-0{\cdot}0790$	$-0{\cdot}1223$	$0{\cdot}0$

The onset of negative values is slightly earlier now. Perturbation of the primary Alfvén wave is worst around $T = 1{\cdot}8$ and is not serious if $0{\cdot}12aU^2/br_m \ll b$, i.e. secondary

effects are negligible if $ar_m^{-1}(U/b)^2 \ll 8$, say. Again the cruder criterion $ar_m^{-1}(U/b) \ll \pi$ (Shercliff 1976) is seen to be too pessimistic, because compensation was neglected. As anticipated, the behaviour with conducting walls is much more acceptable because Δb stays small even as T approaches 2.

Partial compensation between the terms $\partial\Psi/\partial X$ and $\partial\Phi/\partial X$ again includes the suppression of any tendency for any terms to become infinite as $X \to \pm 1$, even when $T = 2$, in this case. Figure 5(*b*) shows how $\Delta b(aU^2/br_m)^{-1}$ varies with T and X, again reaching a reduced maximum (as compared with figure 5*a*) around $T = 1{\cdot}0$ and becoming negative around $T = 1{\cdot}4$. Note the change of scale for negative values. This time, however, the wave velocity perturbation falls to zero at $T \to 2$, and a 'wave' of rapid decrease propagates across the figure after T has passed 1·6. Fairly severe perturbations of the wave persist near $X = \pm 1$ until very late and this could be a source of trouble in practice. It might even be necessary to vary the imposed vertical field or the depth of the sodium tank to allow for this, provided the device was always going to be run at the same energy levels.

We must now briefly re-examine the other aspects of the validity of the linearized approach. Representative secondary velocity and field perturbations are of order aU^2/br_m and $(\mu\rho)^{\frac{1}{2}}aU^2/br_m$ respectively. It is easily verified that we are entitled to neglect the quadratic terms in (4) and (5) if aU^2/br_m is small compared with the wave velocity b and if $(\mu\rho)^{\frac{1}{2}}aU^2/br_m$ is small compared with the imposed field B_0, which is the same condition. Then the contribution of neglected terms such as $\rho v_r \partial v_\theta/\partial r$ to $\rho\,\partial v_\theta/\partial t$ is indeed negligible in times of order a/b (the half transit time). By the same token the distance through which the vorticity is convected is small compared with a in times of this order. Our approach therefore is valid provided only that $ar_m^{-1}(U/b)^2$ is small. It is probable that in a practical device amplitudes would be pushed to the point where this condition was not truly satisfied, even though the slightly less stringent conditions mentioned earlier for securing small perturbation of the primary wave were being satisfied.

6. Events during the downward transit of the primary wave

After T passes the value 2 the primary wave reflects from the top, causing v_θ and B_θ both to fall to zero. It is now a Walén wave (see the introduction), with P zero ahead and behind, and so the primary wave never again generates fresh secondary vorticity. The primary wave stops after this second transit (Shercliff 1976). ω_θ and j_θ henceforth obey the simple wave equations

$$\frac{\mu\,\partial j_\theta}{\partial t} = B_0\frac{\partial \omega_\theta}{\partial z}, \quad \frac{\partial \omega_\theta}{\partial t} = \frac{B_0}{\rho}\frac{\partial j_\theta}{\partial z}. \tag{36}$$

(*a*) *Magnetic-walls case.* Figure 3(*g*) shows the state of the perturbation field at the end of the upward transit of the primary wave. Meanwhile all secondary motion has ceased, for $\omega_\theta = 0$ throughout the fluid while j_θ takes the uniform value $(a^2U^2/2br_m)(\rho/\mu)^{\frac{1}{2}}$ [the residue of the step term S in (20)] plus a current sheet of strength $(-a^3U^2/br_m)(\rho/\mu)^{\frac{1}{2}}$ (the residue of the δ term) at the top wall. Remember that the total azimuthal current has to be zero. At $T = 2$ the top boundary condition (that $\partial\Phi/\partial Z = 0$) is not satisfied, instantaneously, and the result is that the current sheet is reflected

and travels downwards again, but at *constant* strength $(-a^3U^3/br_m)\,(\rho/\mu)^{\frac{1}{2}}$, occupying the same location as the descending primary wave but now not coupled to it. Meanwhile the uniform part of j_θ persists unchanged. With $\omega_\theta = 0$ it is a solution of (36) and may be superposed. The secondary current sheet is inevitably also a vortex sheet, but of opposite circulation to the rising sheet during the first transit, for the wave direction is now reversed. The associated motion is similar to that portrayed in figures 3(*a*)–(*c*), but is reversed, and has different magnitudes for Ψ' because the vortex sheet is now of constant instead of increasing strength. All motion again ceases when the sheets reach the bottom. This is not the end of the matter, however, for now $\partial\Phi/\partial Z \neq 0$ at the bottom and the current sheet travels up again, associated with a secondary motion in the original (first transit) direction. This sequence continues until dissipation of some kind finally intervenes.

(*b*) *Conducting-walls case.* Figures 6(*d*) and (*h*) show the states of the secondary flow and perturbation field at the end of the first transit. Once again a boundary condition is being instantaneously infringed; now we have $v_r \neq 0$ (i.e. $\partial\Psi'/\partial Z \neq 0$) at the top wall, because the vortex sheet has arrived there. The boundary condition will cause this to be reflected and travel downwards without changing sign. In this case it is the associated travelling current sheet which changes sign. Repeated reflexion from bottom and top continues until dissipation intervenes. However, the problem is much more complicated than in the magnetic-walls case and we shall not pursue it further here. The reason is that the waves of vorticity represented by the terms Q' and R' in (28) have now reached the far wall and continue to arrive, so that they participate in satisfying the condition $\partial\Psi'/\partial Z = 0$ at each wall. The result is that the new parts of these waves for $T > 2$ emitted by the bottom and top walls are determined by the old parts still arriving there, along with the contributions to $\partial\Psi'/\partial Z$ of the solution due to the reflected, but now constant, current/vortex sheet and the new harmonic function, which is necessary to allow Ψ' to vanish at the top and bottom.

This behaviour for $T > 2$ would obviously have to be fully investigated before building an Alfvén energy store with conducting walls could be seriously contemplated.

7. The case of primary standing waves

Some interest is attached to the case where the primary Alfvén waves are standing waves rather than progressive waves, e.g. where the Alfvén energy store is acting as a pseudo-capacitor in resonance with an inductive magnetic system. We shall consider only the simplest case that is representative of this class of problems, namely the situation where the waves are merely resonating between the top and bottom walls at $z = 0$ and $2a$, and virtually no power is being exchanged with an external circuit. (At the high Lundquist and Hartmann numbers appropriate to the large Alfvén energy stores under discussion, the effect of dissipation is confined almost entirely to thin Hartmann layers (Shercliff 1965, p. 156) and can be disregarded elsewhere in the primary Alfvén waves, particularly when highly conducting side walls are provided. The same reference discusses various ways in which the dissipated energy could be supplied externally, both at and off resonance. Jameson (1964) describes experiments which exhibit one of the ways in which standing Alfvén waves can be sustained.) The conditions at $z = 0$ and $2a$ will be taken to correspond either to the magnetic-walls case or to the conducting-walls case.

In the magnetic-walls case, the boundary conditions on the primary waves will be $B_\theta = 0$ at $z = 0, 2a$, in the absence of any conductors between the sodium and the magnet poleface, carrying radial currents. In this case the primary standing waves obey equations of the form

$$\left.\begin{aligned} v_\theta &= U\cos(\pi z/2a)\sin(\pi bt/2a) \\ \text{and} \qquad B_\theta &= U(\mu\rho)^{\frac{1}{2}}\sin(\pi z/2a)\cos(\pi bt/2a), \end{aligned}\right\} \tag{37}$$

if we select the fundamental mode, of lowest natural frequency. A radial 'stirring force' F now acts on the fluid in addition to the gradient of p^* and is given by

$$F = \rho\left(v_\theta^2 - \frac{B_\theta^2}{\mu\rho}\right)\frac{1}{r_m} = \rho\frac{U^2}{2r_m}\left(\cos\frac{\pi z}{a} - \cos\frac{\pi bt}{a}\right), \tag{38}$$

in which the unsteady part is irrotational (and will merely be balanced by pressure variations) and the rotational part is steady and will therefore cause a steady secondary motion, which we shall examine.

The conducting-walls case is not very different. The boundary condition is now $v_\theta = 0$ at $z = 0, 2a$, with the result that

$$v_\theta = U\sin(\pi z/2a)\cos(\pi bt/2a),$$

$$B_\theta = U(\mu\rho)^{\frac{1}{2}}\cos(\pi z/2a)\sin(\pi bt/2a),$$

and F is merely the negative of (38), causing secondary flow in the opposite direction.

Returning to the magnetic-walls case, we observe that the main braking mechanism, which yields a *steady* secondary flow in the face of the rotational radial force field F_r, where

$$F_r = (\rho U^2/2r_m)\cos\pi z/a, \tag{39}$$

will be the induction of azimuthal currents j_θ by radial flow across the vertical field B_0. This results in a radial braking force $-\sigma B_0^2 v_r$ because the azimuthal electric field is zero in this axisymmetric configuration. (σ is the electric conductivity.) The fluid being so highly conducting, we shall assume that the secondary flow is slow enough for inertia and viscous forces to be negligible, outside boundary layers at least, and examine these assumptions later. The governing equation is therefore

$$\operatorname{grad} p^{**} = (F_r - \sigma B_0^2 v_r)\,\hat{\mathbf{e}}_r, \tag{40}$$

$\hat{\mathbf{e}}_r$ being the radial unit vector, and p^{**} being p^* less the potential of the irrotational part of F. Equation (40) is linearized, in keeping with the rest of this paper, for not only has the inertia term been omitted but so have the magnetic forces and e.m.f.'s due to the induced, perturbation field. From (40) it follows that $F_r - \sigma B_0^2 v_r$ is independent of z. Integrating from $z = 0$ to $2a$ reveals that in fact

$$F_r = \sigma B_0^2 v_r \quad \text{since} \quad \int_0^{2a} v_r\,dz = 0,$$

in view of flow conservation, and we see that

$$v_r = \frac{\rho U^2}{2r_m\sigma B_0^2}\cos\frac{\pi z}{a}. \tag{41}$$

It follows that $\partial v_z/\partial z = 0$, and in fact $v_z = 0$ from the symmetry about the plane $z = a$.

Equation (41) obviously fails near the side walls, where v_r must fall to zero in boun-

dary layers in which inertial and/or viscous effects must occur. In the case of large Alfvén energy stores running with reasonably large amplitudes it turns out that the boundary layers are inertial. If their thickness is of order δ, the inertia term $\rho(\mathbf{v}.\mathrm{grad})\,\mathbf{v}$ which has to be added to (40) is primarily in the z direction, for $v_r/\delta \approx v_z/a$ (from the equation of continuity). Its curl, due primarily to radial gradients, is of order $\rho a v_r^2/\delta^3$ or $\rho^3 a U^4/\sigma^2 r_m^2 B_0^4 \delta^3$ and must be comparable with the curl of the terms on the right of (40), i.e. of order $\rho U^2/a r_m$. Hence

$$(\delta/a)^3 \approx \rho^2 U^2/a r_m \sigma^2 B_0^4. \tag{42}$$

If we insert the values $\rho = 0{\cdot}93 \times 10^3$, $U = 30$, $a = 2$, $r_m = 8$, η (viscosity) $= 6{\cdot}3 \times 10^{-4}$, $\sigma = 10^7$ and $B_0 = 1$ (all in S.I. units) referred to in the earlier paper (Shercliff 1976) we find that δ takes the relatively small value of 0·016 (i.e. 16 mm).

In the boundary layer the curl of any viscous term introduced into (40) would be of order $\eta v_z/\delta^3$ (η being viscosity) or $\eta a v_r/\delta^4$. As a fraction of the terms that have been retained this is of order $\eta/\rho v_r \delta$. This may be written as $r_m \sigma \eta B_0^2/\rho^2 \delta U^2$, which takes the value $0{\cdot}41 \times 10^{-3}$ with the values given above. Viscosity will evidently be negligible outside Hartmann layers on the top and bottom walls and the viscous sublayers which must exist in the inertial layers. Analysing the nonlinear inertial layers is a very difficult problem and is not necessary for present purposes.

If the primary Alfvén waves are sufficiently weak, however, the secondary-flow boundary layers are viscous rather than inertial and present a linear problem which is easily solved, except in the corners, where the boundary layers intersect with the Hartmann layers. The condition for viscous rather than inertia forces to dominate is that

$$\rho^2 U^2 \delta/\sigma \eta B_0^2 r_m \ll 1, \tag{43}$$

in which the boundary-layer thickness δ is of order $(\eta a^2/\sigma B_0^2)^{\frac{1}{4}}$ or $a/M^{\frac{1}{2}}$ (M being the Hartmann number $aB_0(\sigma/\eta)^{\frac{1}{2}}$), a result misleadingly reminiscent of channel flow and arrived at by making the curl of the viscous terms (of order $\eta a v_r/\delta^4$) comparable with the curl of F_r. In Jameson's (1964) experiments the left-hand side of (43) is approximately 10^{-3} and the boundary layers would be viscous.

The secondary motion consists of a slow cross-flow given by (41), the circulation being completed via the boundary layers on the side walls. The flow is radially outwards near the top and bottom and inwards near the middle in the magnetic-walls case.

It remains merely to consider the perturbation of the magnetic field by the current j_θ, which is given by

$$j_\theta = \sigma B_0 v_r = \pm \frac{\rho U^2}{2 B_0 r_m} \cos \frac{\pi z}{a}. \tag{44}$$

Note that (44) does not depend on the dissipative parameters σ and η. The minus sign corresponds to the magnetic-walls case. The Poisson equation

$$\nabla^2 \phi = -\mu j_\theta$$

is readily solved subject to the usual conditions $\phi = 0$ at $x = \pm a$ and (*a*) $\phi = 0$ or (*b*) $\partial\phi/\partial z = 0$ at $z = 0, 2a$. We find in case (*a*) (conducting walls) that

$$\phi = \frac{8\mu a^2 U^2 \rho}{B_0 r_m \pi^3} \Sigma \frac{\sin(n\pi z/2a)}{n(n^2-4)} \left\{1 - \frac{\cosh(n\pi x/2a)}{\cosh \frac{1}{2} n\pi}\right\} \quad (n \text{ odd and integral})$$

and in case (*b*) (magnetic walls) that

$$\phi = -\frac{\mu a^2 U^2 \rho}{2B_0 r_m \pi^2} \cos\frac{\pi z}{a}\left(1 - \frac{\cosh(\pi x/a)}{\cosh \pi}\right).$$

The alteration of the velocity of the primary Alfvén wave is now due solely to the field perturbations because the secondary velocities (outside the boundary layers) are horizontal and are in any case extremely small. They are at most 5 mm/s in the case discussed earlier (Shercliff 1976). In the magnetic-walls case, in the half nearer the axis, the steady perturbation of the imposed field causes the primary waves to travel faster at the mid-depth and slower near the top and bottom of the torus. The effect is reversed in the half further from the axis. The wave velocity, averaged over the depth, is unchanged. In the conducting-walls case these effects are reversed.

8. Concluding remarks

The main aim here has been to throw some initial light on what appears to be an interesting and potentially important new problem in MHD. The rough estimates of the seriousness of the disruption of the primary Alfvén waves in large energy stores made in the earlier paper have been generally confirmed, but found to be somewhat pessimistic, and the true mechanisms have been elucidated. Choosing conducting walls at the top and bottom results in much less disruption when the waves are progressive. It should be remembered that only a linearized treatment has been given and that to analyse properly the performance of a serious engineering installation the nonlinear effects would have to be explored, as well as the effects of somewhat less idealized boundary conditions, finite conductivity and variable radius (instead of using r_m). The most interesting question still to be investigated is the mechanism of energy transfer from the primary waves to the secondary motions and fields via Coriolis effects.

I am grateful to Mr A. Hulme for arranging the plotting of figures 3 and 6 on a digital computer.

Appendix A. Formulae for computing the conducting-walls case: compound formula for Ψ or Φ

Here the discriminant factor I is $+1$ for Ψ and -1 for Φ. N is $\frac{1}{2}(2n-1)\pi$ (n covering all positive integers), $V = Z - T$ and $W = Z + T - 2$.

Ψ or Φ is found by summing the series

$$\Sigma \frac{(-1)^{n-1}(\cos NX)}{4N^3}(D+E),$$

where

$$D = 2(1-I)\left\{1(\text{if } V<0) + \frac{e^{N(Z-4)} - e^{-NZ}}{1-e^{-4N}}\right\} + e^{NV}(2INZ-1)\,(\text{if } V<0) + e^{-N(W+2)}(\text{if } W \leqslant 0)$$

(D is the part which is acceptable at low or high N) and E must take different forms at low and high N, as follows.

Either (*a*)

$$E(\text{at low } N) = 2[(\sinh^2 N)\exp(NW\coth N)+(\cosh^2 N)\exp(NW\tanh N)]\,(\text{if } W>0)$$
$$+2I[-(\sinh^2 N)\exp(-NV\coth N)+(\cosh^2 N)\exp(-NV\tanh N)]$$
$$-(1+2INZ)e^{-NV}\,(\text{if } V<0)$$
$$+e^{N(W+2)}\,(\text{if } W\leqslant 0)$$
$$+2\{(\sinh^2 N)[I(\sinh N(2-Z))-\sinh NZ]\exp(NT\coth N)$$
$$-(\cosh^2 N)[I(\sinh N(2-Z))+\sinh NZ]\exp(NT\tanh N)\}/\sinh 2N$$

or (*b*)

$$E\ (\text{at high } N) = (2I(NT-1)+1)\,e^{-NV}\,(\text{if } V\geqslant 0)+\tfrac{4}{3}IN^3V^3e^{-N(V+4)}\,(\text{if } V<0)$$
$$+(1-2NW+2N^2W^2+\tfrac{2}{3}N^3W^3(2+NW)\,e^{-4N})\,e^{N(W-2)}\,(\text{if } W>0)$$
$$+(IQ+P)\,e^{-N(V+4)}-[I(2NT-2+Qe^{-4N})+P+(P+R)\,e^{-4N}]\,e^{N(W-2)},$$

in which

$$P=2(1-NT+N^2T^2),\quad Q=\tfrac{4}{3}N^3T^3+2NT-2,\quad R=\tfrac{2}{3}N^3T^3(2+NT).$$

The high-N formula is a truncated series in powers of e^{-4N}.

N.B. Where a term is immediately followed by a condition in parentheses, e.g. '(if $V<0$)', then it is included *only if* the condition is satisfied. The low-N forms are acceptable only for the *first* N, namely $\frac{1}{2}\pi$, for which the high-N form is *not* acceptable.

Appendix B. Formulae for computing Δb, the change in primary step wave velocity

(*a*) *Magnetic-walls case* ($T=2$). The general formula (26) converges very slowly when $T=2$. However we can find a more convenient form, namely

$$\Delta b(aU^2/br_m)^{-1} = \Sigma(-1)^{n-1}\sin NX\left\{\frac{1}{N^2}-\frac{2}{N}-\frac{2}{N}(\coth N-1)\right\}$$
$$=\frac{X}{2}-\frac{2}{\pi}\log\frac{1+\tan(\frac{1}{4}\pi X)}{1-\tan(\frac{1}{4}\pi X)}-4\Sigma\frac{(-1)^{n-1}}{N}\frac{(\sin NX)}{e^{2N}-1}.$$

The average value ($0\leqslant X\leqslant 1$) is given by

$$\Delta b_m(aU^2/br_m)^{-1}=\tfrac{1}{4}-\frac{8G}{\pi^2}-4\Sigma\frac{(-1)^{n-1}}{N^2}\frac{1}{e^{2N}-1},$$

in which G is Catalan's constant (0·915966...).

(*b*) *Conducting-walls case* ($0\leqslant T\leqslant 2$).

$$\Delta b(aU^2/br_m)^{-1}=\Sigma(-1)^{n-1}(Q/2N^2)\sin NX,$$

where

$$Q=2(e^{N(T-4)}-e^{-NT})/(1-e^{-4N})+e^{-2NT}\,(\text{if } T\leqslant 1)$$
$$+\textit{either}\,(\text{if } n=1)\{2[(\sinh^2 N)\exp(NW\coth N)+(\cosh^2 N)\exp(NW\tanh N)]\,(\text{if } T>1)$$
$$-2[(\sinh^2 N)\exp(NT\coth N)+(\cosh^2 N)\exp(NT\tanh N)]\sinh NT/\sinh 2N$$
$$+e^{2NT}(\text{if } T\leqslant 1)\}$$

or (if $n \geqslant 2$) $\{1 + Pe^{-4N} - [P + (P+R)\,e^{-4N}]\,e^{2N(T-2)} + [1 - 2NW + 2N^2W^2 + \frac{2}{3}N^3W^3(2+NW)\,e^{-4N}]\,e^{2N(T-2)}$ (if $T > 1$)$\}$,

in which $P = 2(1 - NT + N^2T^2)$ and $R = \frac{2}{3}N^3T^3(2+NT)$. The average value ($0 \leqslant X \leqslant 1$) is given by $\Delta b_m(aU^2/br_m)^{-1} = \Sigma(-1)^{n-1}Q/2N^3$.

REFERENCES

JAMESON, A. 1964 *J. Fluid Mech.* **19**, 513.

SHERCLIFF, J. A. 1965 *A Textbook of Magnetohydrodynamics*. Pergamon.

SHERCLIFF, J. A. 1976 *Proc. I.E.E.* **123**, 1035.

WALÉN, C. 1944 *Ark. Mat.* A **30**, 15.

WALÉN, C. 1946 *Ark. Mat.* A **33**, 18.